ChemComm

COMMUNICATION

View Article Online
View Journal | View Issue

Cite this: *Chem. Commun.*, 2019, **55**, 2517

Received 7th December 2018,
Accepted 5th February 2019

DOI: 10.1039/c8cc09713e

rsc.li/chemcomm

The atomic structure of a $MgCo_2O_4$ nanoparticle for a positive electrode of a Mg rechargeable battery†

Naoto Kitamura,* Yuhei Tanabe, Naoya Ishida and Yasushi Idemoto

The atomic structure of a spinel-type $MgCo_2O_4$ nanoparticle was investigated by the reverse Monte Carlo modelling using X-ray and neutron total scattering data. It is found that Mg at an octahedral site induces a significant structural distortion, while Mg at a tetrahedral site is considered to move easily to a vacant site. Based on the results, we propose a guideline for the development of a better positive electrode material for a Mg rechargeable battery.

A magnesium rechargeable battery (MRB) can be regarded as one of the most promising candidates for next generation batteries with higher energy density than commercially used lithium-ion batteries (LIBs) because of the difference in the valences of the ionic charge carriers. However, MRBs proposed in previous studies exhibited inferior battery characteristics compared to the current LIBs. For improving the performance of MRBs with a Mg negative electrode, it is mandatory to develop a novel positive electrode material since it determines the achievable energy density basically. Among the reported positive electrode materials,[1–8] $MgCo_2O_4$ with a spinel structure has attracted much attention because of its high theoretical capacity (260 mA h g^{-1} for $MgCo_2O_4 + Mg^{2+} + 2e^- \leftrightarrows Mg_2Co_2O_4$) and high redox potential of Co.[5–8] In general, $MgCo_2O_4$ powder must be nano-sized for rechargeable behaviour since a long diffusion distance of Mg^{2+} within the crystal is not preferable due to the strong electrostatic interaction between Mg^{2+} and O^{2-}. In addition, the atomic structure of the $MgCo_2O_4$ nanoparticle must be clarified in order to develop a novel material with superior positive electrode properties, because the structure should have a significant influence on the Mg insertion/deinsertion into/from the electrode material during discharge/charge cycles. As is well known, however, the nanoparticle does not exhibit prominent Bragg diffraction peaks, and thus the atomic structure of the $MgCo_2O_4$ nanoparticle cannot be determined precisely by structure analysis using the Bragg peaks, such as the Rietveld refinement.

In this study, we performed total scattering measurements on the $MgCo_2O_4$ nanoparticle to visualize its disordered structure, since such a structure cannot be revealed by other experimental methods like nuclear magnetic resonance, extended X-ray absorption fine structure, and so on. Taking the advantage into account, we investigated the atomic structure of the $MgCo_2O_4$ nanoparticle by analyzing total scattering data, and then tried to gain a deeper understanding on the relationship between the atomic structure and the positive electrode properties compared to what is hitherto available in previous studies. We employed the Monte Carlo algorithm where experimental data (total scattering data) were used instead of energy calculation, *i.e.*, the reverse Monte Carlo (RMC) modelling.[9–11]

We synthesized the spinel-type $MgCo_2O_4$ nanoparticle according to a previous work.[6] The metal composition of the sample was determined by inductively coupled plasma (ICP) spectroscopy (ICPE-9000, Shimadzu). We also confirmed that the $MgCo_2O_4$ could work as a positive electrode material by a charge/discharge cycle test (Fig. S1, ESI†).

To reveal the atomic structure of the sample, synchrotron X-ray and neutron total scattering measurements were carried out. The Rietveld refinement (Z-Rietveld program[12]) was performed with the neutron Bragg profile recorded by a backward detector bank of iMATERIA at J-PARC, and then a $3 \times 3 \times 3$ simulation box for the RMC modelling was constructed from the refined unit cell, considering the lowest Q values of the X-ray and neutron total scattering data. An X-ray total scattering pattern was measured with a photon energy of 61.2 keV at the SPring-8 high-energy X-ray diffraction beamline BL04B2.[13] The incident beam intensity was monitored in an ionization chamber filled with Ar gas, and the diffracted X-rays were collected using Ge and CdTe detectors. The obtained pattern was corrected by a standard program.[13] In the case of neutron total scattering, the pattern recorded with a 45° bank of NOVA at J-PARC was normalized into a structure factor $S(Q)$ with background,

Department of Pure and Applied Chemistry, Faculty of Science and Technology, Tokyo University of Science, 2641 Yamazaki, Noda, Chiba 278-8510, Japan.
E-mail: naotok@rs.tus.ac.jp

† Electronic supplementary information (ESI) available. See DOI: 10.1039/c8cc09713e

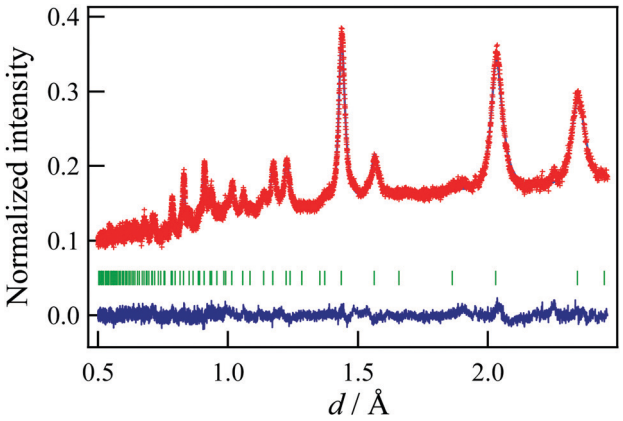

Fig. 1 Rietveld refinement pattern of the $MgCo_2O_4$ nanoparticle (neutron). The red marks and the solid line represent the observed and calculated neutron diffraction intensities, respectively. The vertical marks below the patterns indicate positions of allowed Bragg reflections. The curve at the bottom shows a difference between the observed and calculated intensities.

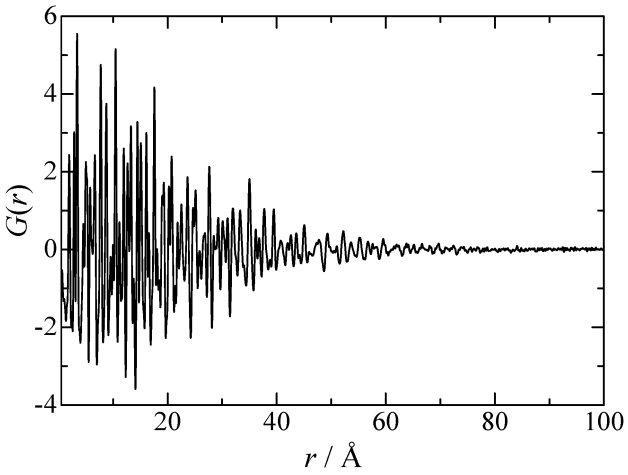

Fig. 2 A reduced pair distribution function of the $MgCo_2O_4$ nanoparticle (X-ray).

V-rod, and empty-can data. These $S(Q)$ data were convolved by taking the size of the simulation box into account, and they are represented as $S_{box}(Q)$ in this paper. The RMC modelling was performed by using the RMCProfile program,[10] and then the simulated snapshot of the atomic configuration was analyzed; that is, polyhedral volumes and distortions were investigated. Based on the obtained results, we discussed the relationship between the structural and electrochemical properties as a positive electrode material for MRB.

Fig. 1 shows the result of the Rietveld refinement using the neutron Bragg profile, and the refined structural parameters are summarized in Table 1. According to previous works,[5–7] we assumed that $MgCo_2O_4$ had a spinel structure, and fixed the Mg : Co ratio taking a result of the ICP measurement into account. As can be seen in Fig. 1, the observed Bragg peaks are considerably broad, suggesting that the particle size of the synthesized $MgCo_2O_4$ is of nano level. It is also found that all the Bragg peaks can be attributed to a spinel structure, and that Mg and Co respectively occupy the octahedral and tetrahedral sites partially. The results indicate that the sample has the "disordered" spinel structure. However, local environment around Mg and Co cannot be distinguished by crystallography, and thus we performed the RMC modelling using the simulation box (1512 atoms) constructed from the unit cell. In the RMC modelling, Mg and Co distributions were determined by swapping Mg and Co in the simulation box, and X-ray and neutron structure factors were fitted simultaneously by optimizing the weighting factors. Fig. 2 shows the X-ray reduced pair distribution function $G(r)$ which was obtained from the structure factor $S(Q)$ by Fourier transform.[14] As can be seen, we can find correlation peaks for the $MgCo_2O_4$ nanoparticle up to 80 Å. The results of the RMC modelling for the $MgCo_2O_4$ nanoparticle are presented in Fig. 3. It can be seen in Fig. 3(a and b) that both the $S_{box}(Q)$ are reproduced well by the modelling.

Table 1 Refined structural parameters of the $MgCo_2O_4$ nanoparticle (space group: $Fd\bar{3}m$). B and g means an atomic displacement parameter and a site occupancy, respectively

Atom	Site	x	y	z	B/Å^2	g
Mg1	8a	0	0	0	4.5(1)	0.494(1)
Co1	8a	0	0	0	= B(Mg1)	0.506(1)
Co2	16d	5/8	5/8	5/8	1.09(4)	0.7411(7)
Mg2	16d	5/8	5/8	5/8	= B(Co2)	0.2589(7)
O	32e	0.38463(5)	= x(O)	= x(O)	1.35(3)	1

Lattice parameter: a = 8.1213(2) Å. R-Factors: R_{wp} = 3.03%, R_p = 2.59%, R_e = 2.27% and S = 1.33.

It is well known that the spinel structure has a vacant octahedral site denoted as 16c site [Fig. 4(a)], which is close to the tetrahedral site (8a site). After discharging MRB using $MgCo_2O_4$ as a positive electrode material, Mg^{2+} is inserted into the vacant site of $MgCo_2O_4$, and then cations at the tetrahedral site are simultaneously pushed out towards the vacant site.[7] As a result, the spinel structure is converted to a rock-salt structure, where the cations occupy both the 16c and 16d sites in the spinel structure [Fig. 4(b)]. Fig. 4(c and d) show a condensed view of $MgCo_2O_4$ which is a time-averaged structure (a crystal structure) constructed from the snapshot of the atomic configuration [Fig. 3(c)]. As can be seen in the figures, cations at the tetrahedral sites spread slightly toward the vacant sites in the nanoparticle. This implies that the phase transition to the rock-salt structure can easily occur in the $MgCo_2O_4$ nanoparticle during the discharging process. Such structural information is considerably hard to be obtained by analysis using only Bragg peaks.

We paid attention on the local environment around Mg and Co in the snapshot of the atomic configuration [Fig. 3(c)], and investigated bond lengths, polyhedral volumes and bond-angle variances (distortions).[16] From the results given in Table 2, it is confirmed that the bond length of Mg–O is longer than that of Co–O, as predicted by a difference in ionic radii between Mg^{2+} and Co^{3+}.[17] Furthermore, it is found that the distortion around Mg at the octahedral site is larger than that around Co at the same crystallographic site. Since the cations at this site can be regarded as pillars of the spinel structure, it is considered that the Mg amount at the octahedral site should be decreased for

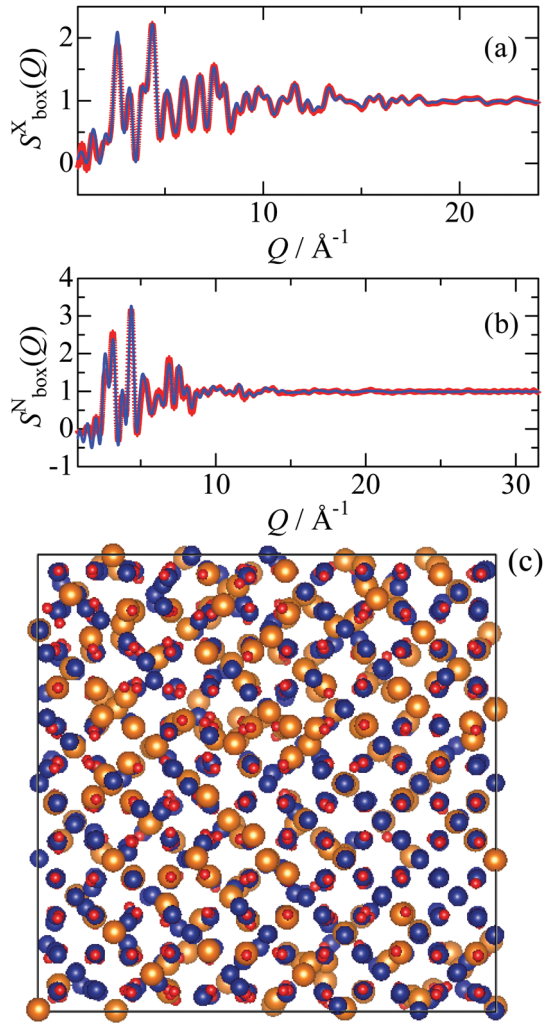

Fig. 3 (a) X-ray and (b) neutron structure factors of the $MgCo_2O_4$ nanoparticle. The red marks and the blue solid line represent the experimental data and RMC model, respectively. (c) Atomic-configuration snapshot of $MgCo_2O_4$. The snapshot was visualized by a VESTA program.[15] Color code: Mg, orange; Co, blue; and O, red.

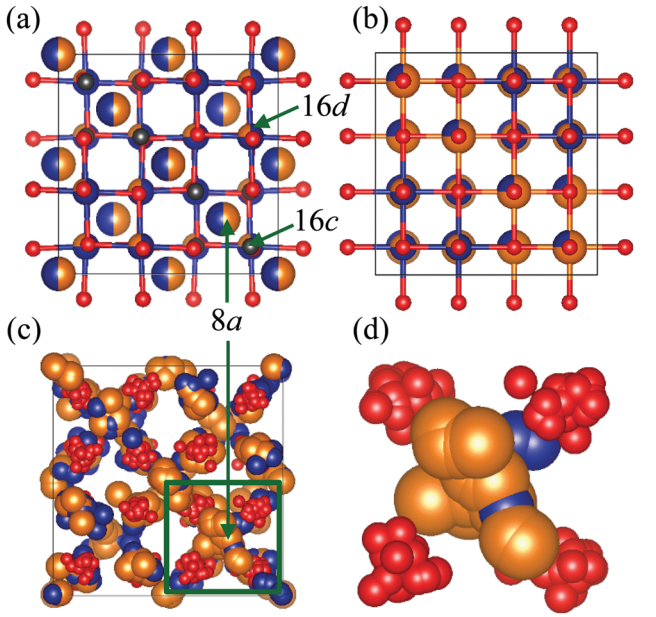

Fig. 4 (a) A refined unit cell of $MgCo_2O_4$ with the disordered spinel structure. Gray small spheres represent the vacant site (16c site). (b) The rock-salt structure after discharging. (c) A condensed view of $MgCo_2O_4$ constructed using the RMC modelling and (d) the enlarged view within a green square of (c). Color code: Mg, orange; Co, blue; and O, red.

Table 2 Bond lengths of Mg–O and Co–O, and bond-angle variances σ^2 of polyhedra in the $MgCo_2O_4$ nanoparticle

Polyhedron	Bond length/Å	Bond angle variance/deg.^{2}
MgO_6	2.085	157.7
CoO_6	1.978	115.2
MgO_4	1.969	196.6
CoO_4	1.830	118.5

Table 3 Volume around the vacant site (16c site), and MgO_6 and CoO_6 volumes in the $MgCo_2O_4$ nanoparticle

Octahedron	Volume/Å^3
Vacancy (16c)-O_6	12.16
MgO_6	11.22
CoO_6	9.77

stable positive electrode properties. In other words, a disorder in the spinel structure of $MgCo_2O_4$ should be suppressed.

Table 3 compares the volume around the vacant site (16c site) to MgO_6 and CoO_6 volumes in the $MgCo_2O_4$ nanoparticle with the disordered spinel structure. An important finding noted in this table is the fact that the volume around the vacancy is almost equal to the MgO_6 volume. This result indicates that Mg^{2+} at the tetrahedral site (8a site) can move to the vacant site more easily compared to Co^{3+} at the tetrahedral site, due to the smaller volume mismatch. From this viewpoint, it is also considered that the disorder in the spinel structure must be suppressed, to facilitate the phase change from the spinel structure to the rock-salt structure during the discharging process.

Based on these analytical results, a partial substitution of Co by Mn can be regarded promising, since $MgMn_2O_4$ has an ordered spinel structure (a normal spinel structure).[6] Indeed, the Mn-substituted sample showed higher discharge capacity in comparison to the pure $MgCo_2O_4$, as reported elsewhere.[18] It is also useful to choose another cation (M) which can be expected to form MO_6 with the same volume as the vacant site.

In this work, we focused on a $MgCo_2O_4$ nanoparticle, which is one of the most promising candidates for a positive electrode material of MRB. A structural investigation employing the reverse Monte Carlo modelling could reveal the cation distribution, polyhedral distortions, and local environment around the vacancy successfully. Based on these results, a guideline for the development of a novel positive electrode material was proposed.

This study is supported partially by the Advanced Low Carbon Technology-Specially Promoted Research for Innovative Next Generation Batteries Program (ALCA-SPRING) of Japan Science and Technology Agency (JST). We are grateful to Dr K. Ohara (JASRI)

for his support with X-ray total scattering measurement at SPring-8, Japan (Proposal No. 2018B1260). We also thank Profs T. Otomo, K. Ikeda (KEK), T. Ishigaki and A. Hoshikawa (Ibaraki Univ., Japan) for their support with neutron total scattering measurements at J-PARC, Japan (No. 2018A0011 and 2017PM0006). Discussion with Dr S. Kohara (NIMS) is gratefully appreciated.

Conflicts of interest

There are no conflicts of interest to declare.

Notes and references

1 D. Aurbach, Z. Lu, A. Schechter, Y. Gofer, H. Gizbar, R. Turgeman, Y. Cohen, M. Moshkovich and E. Levi, *Nature*, 2000, **407**, 724.
2 M. M. Huie, D. C. Bock, E. S. Takeuchi, A. C. Marschilok and K. J. Takeuchi, *Coord. Chem. Rev.*, 2015, **287**, 15.
3 Y. Orikasa, T. Masese, Y. Koyama, T. Mori, M. Hattori, K. Yamamoto, T. Okado, Z. Huang, T. Minato, C. Tassel, J. Kim, Y. Kobayashi, T. Abe, H. Kageyama and Y. Uchimoto, *Sci. Rep.*, 2014, **4**, 5622.
4 N. Ishida, R. Nishigami, N. Kitamura and Y. Idemoto, *Chem. Lett.*, 2017, **46**, 1508.
5 T. Ichitsubo, T. Adachi, S. Yagi and T. Doi, *J. Mater. Chem.*, 2011, **21**, 11764.
6 S. Yagi, Y. Ichikawa, I. Yamada, T. Doi, T. Ichitsubo and E. Matsubara, *Jpn. J. Appl. Phys.*, 2013, **52**, 025501.
7 S. Okamoto, T. Ichitsubo, T. Kawaguchi, Y. Kumagai, F. Oba, S. Yagi, K. Shimokawa, N. Goto, T. Doi and E. Matsubara, *Adv. Sci.*, 2015, **2**, 1500072.
8 Y. Kotani, R. Ise, K. Ishii, T. Mandai, Y. Oaki, S. Yagi and H. Imai, *J. Alloys Compd.*, 2018, **739**, 793.
9 R. L. McGreevy and L. Pusztai, *Mol. Simul.*, 1988, **1**, 359.
10 M. G. Tucker, D. A. Keen, M. T. Dove, A. L. Goodwin and Q. Hui, *J. Phys.: Condens. Matter*, 2007, **19**, 335218.
11 N. Kitamura, *J. Ceram. Soc. Jpn.*, 2015, **123**, 637.
12 R. Oishi, M. Yonemura, Y. Nishimaki, S. Torii, A. Hoshikawa, T. Ishigaki, T. Morishima, K. Mori and T. Kamiyama, *Nucl. Instrum. Methods Phys. Res., Sect. A*, 2009, **600**, 94; R. Oishi-Tomiyasu, M. Yonemura, T. Morishima, A. Hoshikawa, S. Torii, T. Ishigaki and T. Kamiyama, *J. Appl. Crystallogr.*, 2012, **45**, 299.
13 S. Kohara, M. Itou, K. Suzuya, Y. Inamura, Y. Sakurai, Y. Ohishi and M. Takata, *J. Phys.: Condens. Matter*, 2007, **19**, 506101.
14 D. A. Keen, *J. Appl. Crystallogr.*, 2001, **34**, 172.
15 K. Momma and F. Izumi, *J. Appl. Crystallogr.*, 2011, **44**, 1272.
16 K. Robinson, G. V. Gibbs and P. H. Ribbe, *Science*, 1971, **172**, 567.
17 R. D. Shannon, *Acta Crystallogr., Sect. A: Cryst. Phys., Diffr., Theor. Gen. Crystallogr.*, 1976, **32**, 751.
18 Y. Idemoto, Y. Mizutani, C. Ishibashi, N. Ishida and N. Kitamura, to be submitted.

